

Numerical Investigation of PCM Thermal Storage in Water Solar Collector

Open
Access

Kadhim Hussein Suffer^{1,*}, Jalal M. Jalil², Hiba A. Hasan³

¹ Mechanical Engineering Dept., Engineering College, Al-Nahrain University, P.O. Box 64040, Baghdad, Iraq

² Electromechanical Engineering Dept., University of Technology, Baghdad, Iraq

³ Computer Techniques Engineering Dept., Al-Turath University College, Baghdad, Iraq

ARTICLE INFO

Article history:

Received 1 November 2019

Received in revised form 14 December 2019

Accepted 5 January 2020

Available online 26 February 2020

ABSTRACT

Phase Change Materials (PCMs) mainly used for Thermal energy storage. Computational Fluid Dynamics (CFD) is used to investigate numerically the temperature distribution over the time for water flowing inside the pipes of solar collector and the PCM placed on the back layer of the collector as a storage media. Phase change problems were solved using the general governing equation for energy. The finite volume method and the proposed enthalpy conversion model were used for the mathematical model of PCM. The simulation results give that the maximum outlet water temperature is (58 °C) at (4:00 PM), while the maximum temperature of PCM is (54 °C) at (5:00 PM). The water temperature is higher than that PCM temperature at the day hours (PCM Charge). The PCM temperature close to the water temperature at the time (5:30 PM). The average temperature of PCM is always reached required temperature (34 °C) except time (8:00 AM), this means that the PCM is capable to charge the water with the required energy during the night. The predicted results from CFD gives a good agreement with the experimental results that which is studied and published previously.

Keywords:

Renewable Energy; Thermal Energy
Storage; PCM; Enthalpy Method

Copyright © 2020 PENERBIT AKADEMIA BARU - All rights reserved

1. Introduction

Increased combustion of fossil fuels resulting from increased energy consumption in our world leads to increased emission of carbon dioxide and increase environmental pollution and global warming. These reasons led to seeking other energy sources, and therefore renewable energy sources, primarily solar energy are an appropriate solution to these problems. Since the solar energy is not continuous and has low intensity, therefore there are many researchers who are a focus and interested in the possibility of storing energy from time, which that energy available to use on the other time, such as solar energy. Thermal Energy Storage (TES) balances energy consumption and energy production [1]. TES classified into three main categories: sensible heat TES, latent heat TES and thermochemical energy TES [2].

* Corresponding author.

E-mail address: kadhim_askar@yahoo.com (Kadhim Hussein Suffer)

Latent heat TES is the most effective technique because of its high heat storage capacity within a nearly constant range of temperature corresponding to the phase change temperature of the storage material [3]. Phase change materials (PCMs) are the materials used in the latent heat TES, PCMs have been used in many applications [4]. Jalil *et al.*, [5] presented an experimental and numerical study of the process of ice melting as PCMs around a horizontal cylinder for proposing of thermal storage in one of air conditioning applications. In solar heating systems, PCMs were used with different fabrication techniques. For example, Reddy [6] constructed a system consists of two rectangular containers, PCMs was placed in the top container, while water was placed in the bottom container; Prakash *et al.*, [7] studied a layer of capsules filled with PCM used to heat water in the storage; Jalil *et al.*, [8] performed an experimental study in lab conditions with different heat flux for improving the thermal performance of the solar collector by using paraffin wax as a PCMs. From that experiment, they found that the water temperature is to become higher than 35 °C until the next day with high load conditions. The temperature of 10 °C and 6 °C increases in thermosiphon and the water tank respectively at the increasing of 33.3% heat flux. Yue Hu *et al.*, [9] presented numerical and experimental study to develop to maximize the use of solar energy with PCMs for pre-heat the ventilated air in an air heat exchanger integrated with a ventilated window. Vikram *et al.*, [10] investigated the thermal performance and feasibility of TES with PCM (paraffin) embedded in cylindrical aluminum capsules, for heating water for domestic motivations, the results indicated that the proposed system was a commercially feasible choice for solar. PCMs of stearic acid and hydrated salt $\text{CaCl}_2\cdot 6\text{H}_2\text{O}$ within the TES system with a solar still and beneath a collector, have been studied by El-Sebaï *et al.*, [11] and Koca *et al.*, [12], respectively. Chen *et al.*, [13] structured a solar flat-plate collector with paraffin-embedded in aluminum foam and concluded significant improvement in the heat transfer performance of the collector. Wu *et al.*, [14] inserted an oscillating heat pipe (OHP) and PCMs in an experimental study to improve the performance of a novel solar water heating system. They have carried out the experimental test for the full-year measurement in different environmental conditions in Nanjing city of China. They concluded that the proposed system is provided to be effective and help in a solar energy application. Gracia *et al.*, [15] concluded that the use of the domestic electrical hot water cylinder with 57 vertical pipes filled with PCM increased the capacity of TES and reduced the cost of electricity. Khote [16] used spherical capsules filled with HS-58 PCM to improve the TES system for heating water in solar domestic applications, the results showed that the used system was economical and the enhancement was 22% in thermal storage capacity. Redzuan *et al.*, [17] developed a 3D CFD model for solar water heater integrated with PCM used in domestic and commercial applications, the simulation results showed that the developed model can be used as a research predictor to reduce the cost of the solar collector experimental rig. Prakash *et al.*, [18] proposed a design, integration and real environment investigation for an off-grid solar thermal water heating system by using PCMs. Paraffin wax, stearic acid/palmitic acid eutectic and puretemp68 mixture used as PCMs in a designed heat storage tank. They are founding that the efficiency of water charging from stearic acid/palmitic acid (55%) is higher compared to that from paraffin wax (20%) and better than puretemp68 (45%). Bazri *et al.*, [19] investigated the latent heat storage tank filled with paraffin wax and the tank was connected to the compact design of evacuated heat pipe solar water heater, the system performance was studied for different flow rates, different climatic condition, and different PCMs, the results indicated that suggest system improved the average efficiency from nearly 10% to 58% compared with the conventional system, for different PCMs. Sidik *et al.*, [20] and Kean and Sidik [21] studied the using of nanofluid PCM to enhance the performance of cold TES. Mohamad *et al.*, [22] employed the PCM ($\text{CaCl}_2\cdot 6\text{H}_2\text{O}$) to characterize the phase change temperature and supercooling degree by the addition of different volume fraction of graphene nanoplatelets (GNP). Pushpendra [23] studied experimentally the thermal performance of solar

water heater at different flow rates with and without cylinder contain organic and spiral copper tubes, the results showed that the thermal performance and heat-storing capacity of the solar water heater was improved with PCM cylinder and thus assure saving of energy. Bouhal *et al.*, [24] compared numerically between two codes to investigate the improvement of solar water heaters working cycle by encapsulated PCM for DHW applications, these codes were built to simulate the phase transition phenomena of PCM under a realistic climate zone (Marrakech, Morocco), the first code was used the Enthalpy method while the second based on the technique of apparent heat capacity.

The main aim of the present study is to investigate numerically the temperature distribution with the time for the solar water collector by using paraffin wax (PCM) to store thermal energy. The temperature distribution will be carried out for both water flowing inside the collector pipes and the paraffin wax placed on the back layer of the collector. The solar collector proposed in this simulation is designed and experimentally investigated by a previous study [25] for determining the temperature distribution over time.

2. Formulation of the Physical Problem

Figure 1 shows the schematic diagram and the details for the solar collector, while Figure 2 shows the schematic diagram, while (Section A–A in Figure 1) present the paraffin wax filled in the container at the back of the collector pipes; physical properties and mass of the paraffin wax are tabulated in Table 1. The paraffin wax used in the previous experimental test is the soft paraffin wax that is produced by the Iraqi Ministry of Oil (refinery Dora). The reason to choose this wax, it is available and cheap compared to imported wax, also it has a low melting point, so it can be used throughout the year, especially in winter days when temperatures drop.

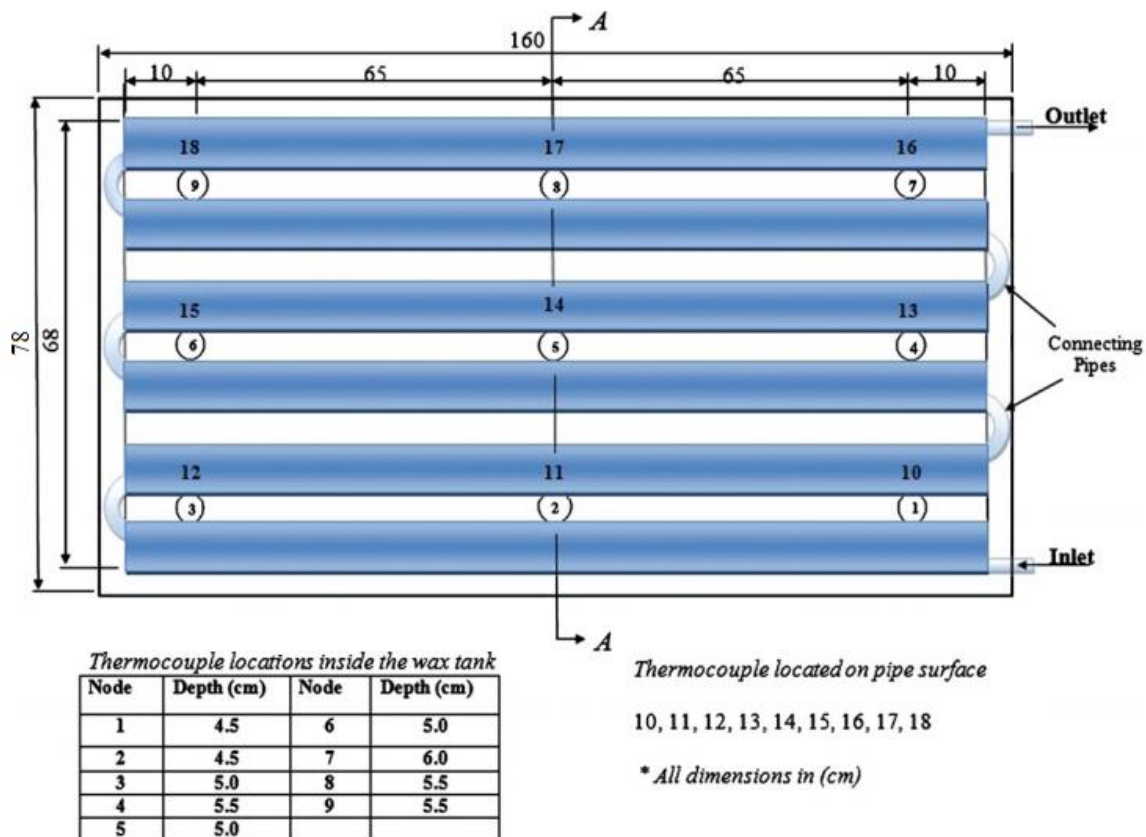


Fig. 1. Schematic diagram of the front view for the storage solar collector

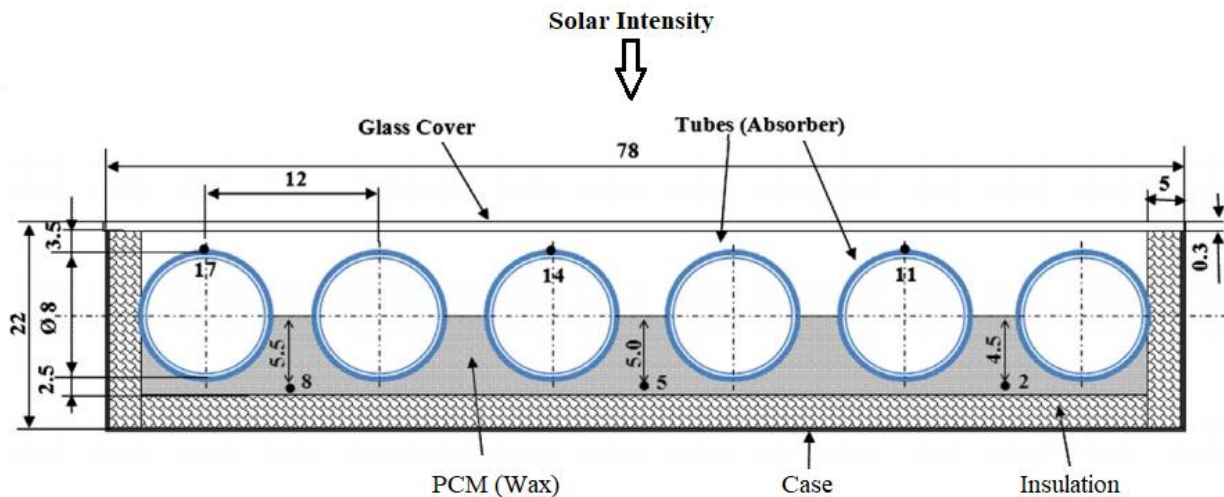


Fig. 2. Section A-A in Figure 1 showing the location of the paraffin wax at the back layer

Table 1

Physical properties and mass of the paraffin wax

Property	Value
Density	970 kg/m ³
Thermal conductivity	0.23 W/m °C
Specific heat capacity	2.890 kJ/kg °C
Latent heat	2.244 kJ/kg
Melting point	46.7 °C
Total mass	42.4 kg

The aim of the present work is to study numerically the distribution of temperature over time for paraffin wax at the back layer of the storage solar collector. The solar intensity of the whole day applies to the upper surface of the solar collector and then transferred as solar energy (q_{solar}) to warm the water in pipes and stored in paraffin wax as thermal energy stored. Figure 3 illustrates the domain of the numerical simulation of the current physical problem with the details and the control volume portion of a three-dimensional in a Cartesian coordinate.

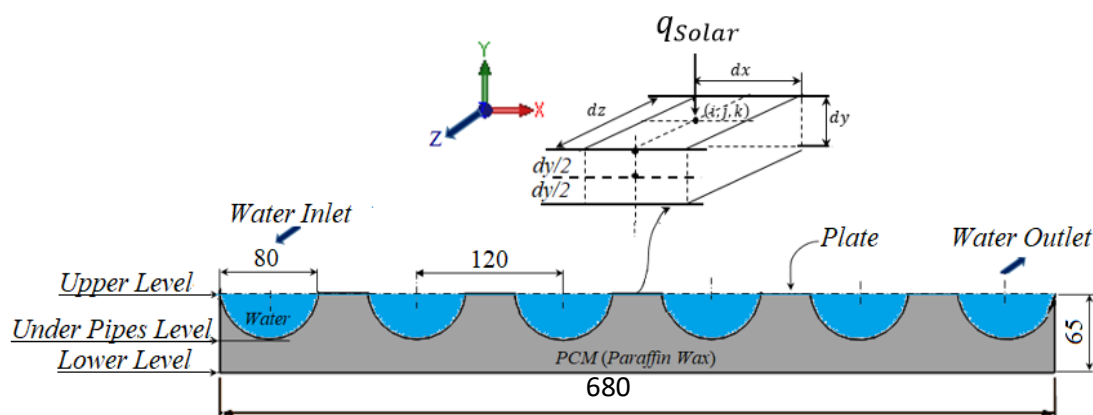


Fig. 3. The domain of the numerical simulation of the current physical problem (all dimensions in mm)

In this simulation, the obtained results from the previous experimental work are used as boundary conditions. The previous experimental work is conducted for the heating system at the latitude 33.3°N of the capital city of Iraq (Baghdad) in (winter season), it is titled of 45° and oriented due south. The average speed of the air was 3.3 m/s and relative humidity is about 50 % are measured using model 8901 Vane Thermo-Anemometer with accuracy ±2%. The temperatures at various locations in the heating system were measured by calibrated K- type thermocouples connected to a temperature recorder (TM-925), the accuracy of this device is in the range of 0.1°C for the temperature measurements between -50.0 to 1300.0 °C ± (0.4% + 0.8°C). Experimental work was carried out for nine sunshine hours and the solar intensity is measured using the Daystar solar meter has an accuracy of 3% for a range from 0 - 1200 W/m² with a resolution of 1 W/m². The measured solar intensity found in the range of 500- 600 W/m² in the morning 8:00 AM, and increase to 830 W/m² in peak time, and then decreases to 100 W/m² in the afternoon at 5:00 PM. The interpolation between inlet and outlet temperature over time for each pipe used as a boundary condition.

The total energy added to the paraffin wax is equal to the total energy transferred from the water flowing inside the pipes crossing the pipe wall then to the paraffin wax, and the solar intensity transmitted through copper welded plates between the pipes. Formulation of the physical model for the paraffin wax (phase change material) is supposed to be unsteady conduction of the energy storage, in addition, to assume the paraffin wax is isotropic and homogenous.

The following equations are used to calculate the temperature with the time for the paraffin wax, the energy balance for the plates between the pipes represented by the following equations.

$$q_{solar} d_x d_z + \left(\frac{k_c d_x d_z (T_{i,j-1} - T_{i,j})}{\Delta y} \right) = \rho_c C p_c \Delta x \Delta y \Delta z \frac{T_{i,j}^{P+1} - T_{i,j}^P}{\Delta t} \quad (1)$$

where; T is the temperature in (°C), (i,j,k) are the unit vectors; (c) represent slabs metal (copper); p is the time. By Simplification

$$T_{i,j}^{P+1} = T_{i,j}^P + \frac{\Delta t}{\rho_c C p_c \Delta y} [q_{solar} + k_c (T_{i,j-1} - T_{i,j})] \quad (2)$$

2.1 Balancing Equation for Latent Storing Energy

The enthalpy transformation method used to formulate the mathematical model for the paraffin wax, and the general energy equation has presented the relationship between the temperature and the enthalpy. Neglecting both of the viscous dissipation and the convective terms. The following equations are representing the model of the general three-dimensional energy equation that was funded by Cao [26].

$$\frac{\partial}{\partial x} \left(k \frac{\partial T}{\partial x} \right) + \frac{\partial}{\partial y} \left(k \frac{\partial T}{\partial y} \right) + \frac{\partial}{\partial z} \left(k \frac{\partial T}{\partial z} \right) + \bar{q} = \rho \frac{\partial H}{\partial t} \quad (3)$$

And the state equation,

$$\frac{\partial H}{\partial T} = C_p \quad (4)$$

The heat capacity for each phase is analogous, and the phase change takes place at a fixed temperature,

$$T = \begin{cases} T_{melt} + H/C_{ps} & , H \leq 0 & \text{(solid phase)} \\ T_{melt} & , 0 < H < L & \text{(phase change)} \\ T_{melt} + (H - L)/C_{pl} & , H \geq L & \text{(liquid phase)} \end{cases} \quad (5)$$

Supposing the paraffin wax is in the solid phase at $H=0$, and Kirchhoff temperature is displayed as

$$T^* = \int_{T_m}^T k(\eta) d\eta = \begin{cases} k_s(T - T_{melt}), & T < T_{melt} \\ 0, & T = T_{melt} \\ k_l(T - T_{melt}), & T > T_{melt} \end{cases} \quad (6)$$

By using definition of the Eq. (17), Eq. (16) can be converted as

$$T^* = \begin{cases} k_s H/C_{ps} & , H \leq 0 \\ 0, & 0 < H < L \\ k_l (H - L)/C_{pl} & , H \geq L \end{cases} \quad (7)$$

Therefore, the enthalpy function can be presented as

$$T^* = \lambda(H)H + S(H) \quad (8)$$

$$\lambda(H) = \begin{cases} k_s/C_{ps} & , H \leq 0 \\ 0, & 0 < H < L \\ k_l/C_{pl} & , H \geq L \end{cases} \quad (9)$$

and,

$$S(H) = \begin{cases} 0, & H \leq 0 \\ 0, & 0 < H < L \\ -Lk_l/C_{pl} & , H \geq L \end{cases} \quad (10)$$

By superseding Eq. (8) in Eq. (3) gives

$$\rho \frac{\partial H}{\partial t} = \frac{\partial}{\partial x} \left(\frac{\partial(\lambda H)}{\partial x} \right) + \frac{\partial}{\partial y} \left(\frac{\partial(\lambda H)}{\partial y} \right) + \frac{\partial}{\partial z} \left(\frac{\partial(\lambda H)}{\partial z} \right) + p + q \quad (11)$$

With

$$p = \frac{\partial}{\partial x} \left(\frac{\partial S}{\partial x} \right) + \frac{\partial}{\partial y} \left(\frac{\partial S}{\partial y} \right) + \frac{\partial}{\partial z} \left(\frac{\partial S}{\partial z} \right) \quad (12)$$

Eq. (11) can be reduced to the following formula in the liquid region

$$\rho \frac{\partial H}{\partial t} = \frac{\partial}{\partial x} \left(k_l \frac{\partial T}{\partial x} \right) + \frac{\partial}{\partial y} \left(k_l \frac{\partial T}{\partial y} \right) + \frac{\partial}{\partial z} \left(k_l \frac{\partial T}{\partial z} \right) + q \quad (13)$$

While in the solid region, Eq. (13)-(15) can be reduces to following formula:

$$\rho \frac{\partial H}{\partial t} = \frac{\partial}{\partial x} \left(k_s \frac{\partial T}{\partial x} \right) + \frac{\partial}{\partial y} \left(k_s \frac{\partial T}{\partial y} \right) + \frac{\partial}{\partial z} \left(k_s \frac{\partial T}{\partial z} \right) + q \quad (14)$$

For the region of the paraffin wax, with no-convection term Eq. (12) can be presented as

$$\rho \frac{\partial H}{\partial t} = \frac{\partial^2}{\partial x^2} (\lambda H) + \frac{\partial S^2}{\partial x^2} + \frac{\partial^2}{\partial y^2} (\lambda H) + \frac{\partial S^2}{\partial y^2} + \frac{\partial^2}{\partial z^2} (\lambda H) + \frac{\partial S^2}{\partial z^2} \quad (15)$$

And for $\lambda = \lambda H$, and $S = S(H)$, the finite-volume method with an explicit scheme is used to evaluate the above equations as

$$\iiint_{\Delta V} \rho \frac{\partial H}{\partial t} = \rho \Delta V \left(\frac{H_p - H_p^\circ}{\Delta t} \right) \quad (16)$$

After this, the Eq. (11) can be written in the standard formula as

$$a_P H_P = a_N H_N + a_S H_S + a_E H_E + a_W H_W + a_T H_T + a_B H_B + b$$

$$a_P = a_N + a_S + a_E + a_W + a_T + a_B$$

$$a_E = \frac{\Delta t}{\rho \Delta V} \frac{\lambda_E A_x}{\delta x_e}, a_W = \frac{\Delta t}{\rho \Delta V} \frac{\lambda_W A_x}{\delta x_w}, a_N = \frac{\Delta t}{\rho \Delta V} \frac{\lambda_N A_y}{\delta y_n}, a_S = \frac{\Delta t}{\rho \Delta V} \frac{\lambda_S A_y}{\delta y_s}, a_T = \frac{\Delta t}{\rho \Delta V} \frac{\lambda_T A_z}{\delta z_t}, a_B = \frac{\Delta t}{\rho \Delta V} \frac{\lambda_B A_z}{\delta z_b}$$

$$A_x = \Delta y \Delta z, A_y = \Delta x \Delta z, A_z = \Delta x \Delta y, \Delta V = \Delta x \Delta y \Delta z \quad (17)$$

and,

$$b = -[a_N + a_S + a_E + a_W + a_T + a_B - 1]H_p^\circ + b_N S_N + b_S S_S + b_E S_E + b_W S_W + b_T S_T + b_B S_B - b_P S_P + \frac{dt}{\rho} q \Delta V \quad (18)$$

For H at grid point P , H_p° is present to the old value, and the values of the coefficients becomes as

$$b_P = b_N + b_S + b_E + b_W + b_T + b_B \quad (19)$$

$$b_E = \frac{\Delta t}{\rho \Delta V} \frac{A_x}{\delta x_e}, b_W = \frac{\Delta t}{\rho \Delta V} \frac{A_x}{\delta x_w}, b_N = \frac{\Delta t}{\rho \Delta V} \frac{A_y}{\delta y_n}, b_S = \frac{\Delta t}{\rho \Delta V} \frac{A_y}{\delta y_s}, b_T = \frac{\Delta t}{\rho \Delta V} \frac{A_z}{\delta z_t}, b_B = \frac{\Delta t}{\rho \Delta V} \frac{A_z}{\delta z_b} \quad (20)$$

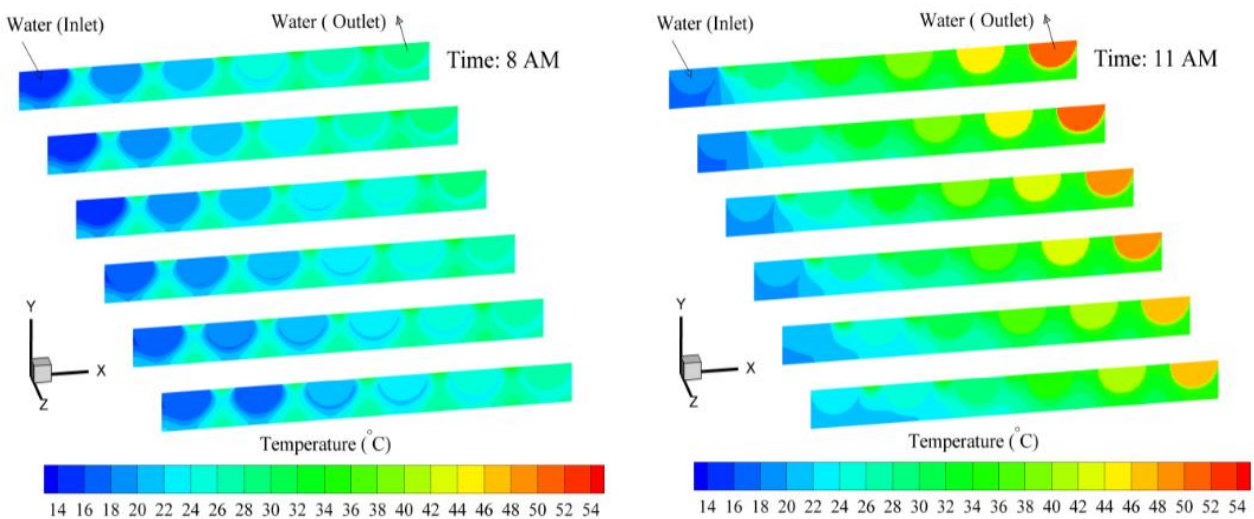
The mesh size of each paraffin wax rectangular encapsulation is (3283200) in (x, y, and z) directions. Transient governing equation and the Finite Volume Method (FVM) under the explicit scheme over a control volume is used to solve the physical problem, which was carried in a subroutine for the charging time is (24 Hr.) with 10 second as a time step in solving the distribution of temperature in the paraffin wax region.

2.2 Initial Conditions

Initially, the solar intensity (q_{solar}), inlet and outlet water temperature (T_{win} and T_{wout}) from the previous experimental work for a clear day on February (2010). Temperature of the environment was (25°C), freezing and melting temperature of paraffin wax are (30°C and 35°C) respectively, time step is (10 sec.), and maximum time (24 Hr.) where used as initial conditions in the present simulation.

3. Results and Discussions

The computer program was built to perform all calculations with the help of initial and boundary conditions. Figure 4 to 6 show the contours of the temperature distribution results conducted from the numerical simulation. Figure 4 shows the contours of the temperature distribution at different local time in (x, y) plane for a different section in the z-direction. The boundary conditions of the calculation are the water temperature through the pipes that it's taken from experimental results [18]. As shown in Figure 4, the temperature of the water is increased from inlet to outlet. The paraffin wax temperature is increasing as the temperature of water increases and it increases as solar intensity increases. The temperature of the paraffin wax will be between inlet and outlet water temperature as shown in figure. Also, the temperature of the paraffin wax increases close to the pipes of water and the plates between the pipes. From Figure 4, selected points at the inlet and outlet of the pipe collector were chosen for water temperature and selected points were chosen for the temperature of paraffin wax directly under the selected points for the water to be plotted in Figure 5. The chosen points represent the periodic change of temperature during the day. The scale of the x-axis in Figure 5 refers to the time starting from (8:00 AM) and so on. From Figure 4 and 5, it can be observed that the maximum outlet water temperature is 58 °C, it occurs at the peak of the solar intensity at the time (4:00 PM), while the maximum temperature of paraffin wax occurs at time (5:00 PM) in the position directly in lower level under the pipe at exit is equals to 54 °C. From graphs of Figure 4 and 5, it can be noted that the temperature of the water is higher than that paraffin wax temperature at the morning hours until the peak time (Paraffin wax charging), the water and wax graphs are close together at (5:00 PM), then the wax graph start to become higher than the water graph until early morning of the next day, (Paraffin wax discharging).



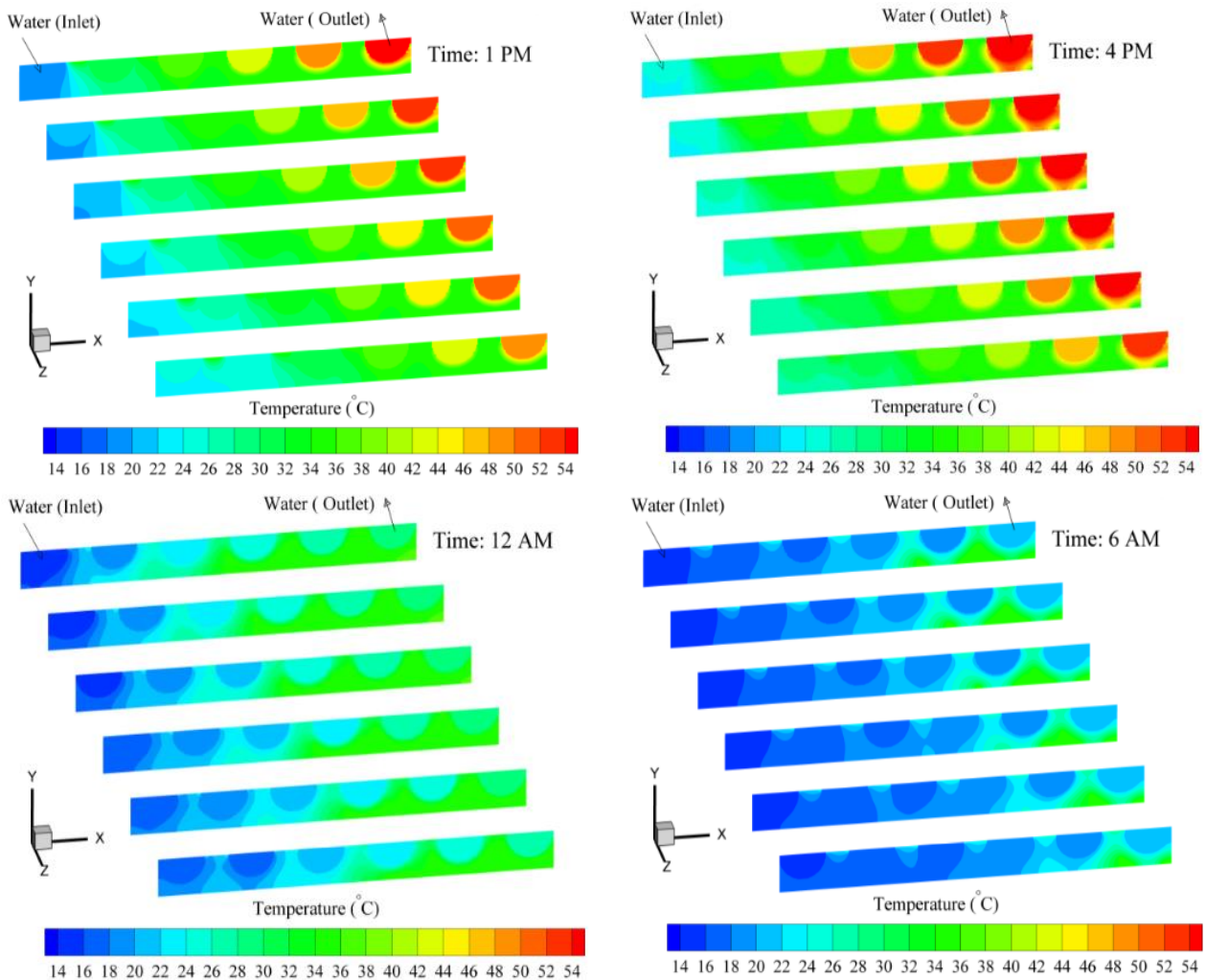


Fig. 4. Contours of the temperature distribution at different time in (x, y) plane with different sections in z -direction

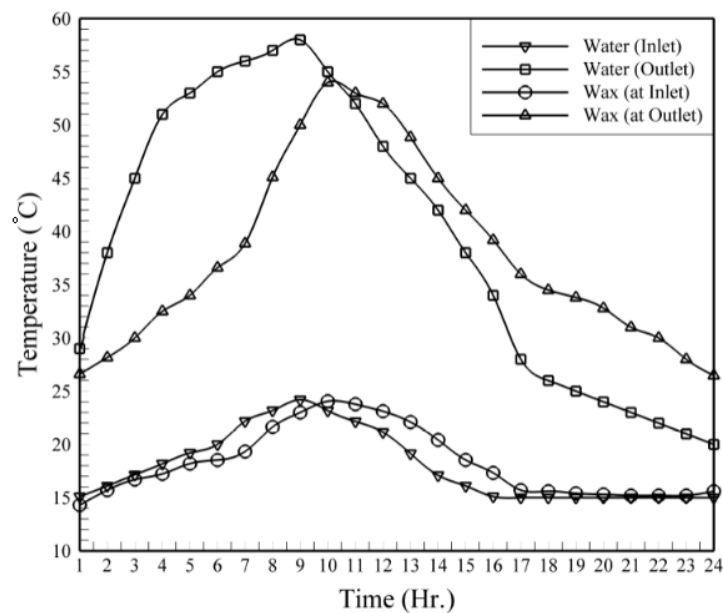


Fig. 5. Variations of the temperature with the day hours in the water and PCM (paraffin wax) at inlet and outlet solar collector

Figure 6 shows the contours of the temperature distribution in y-z plane with different sections in the x-direction. From the sections of this contours, it can be shown that the increase in the temperature of paraffin wax and water from the entrance to the exit. It is clear that it can be seen that the maximum temperature of water at peak time (4:00 PM) at the pipe exit.

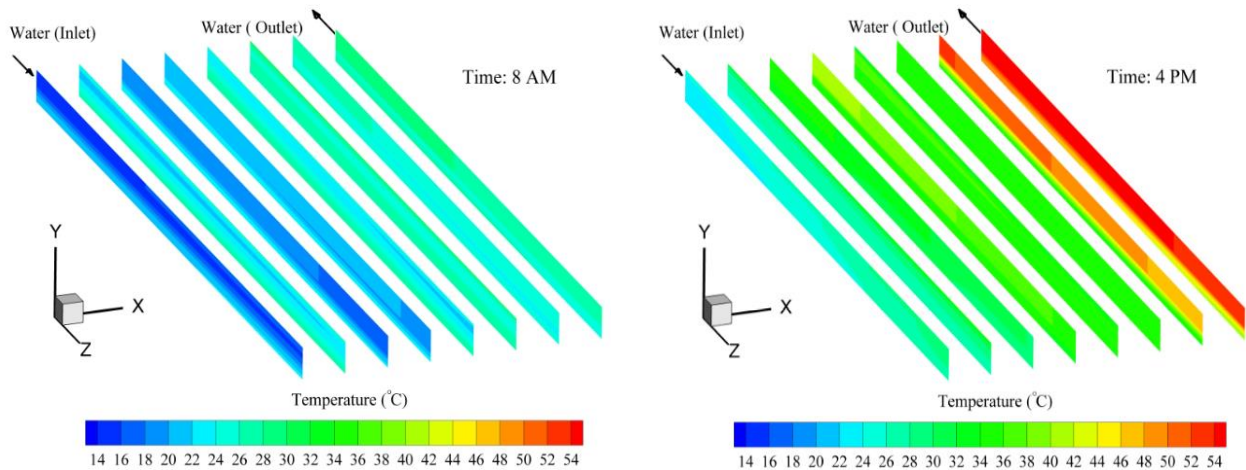


Fig. 6. Contours of the temperature distribution at different time in (y, z) plane with different section in x-direction

Figure 7 presents the temperature distribution in x-z plane of the three selected levels in y-direction of the solar collector, (Upper level at $y = 65$ mm, under pipes level at $y = 22$ mm, and lower level at $y = 2$ mm). In the upper level, the figure shows the temperatures of Paraffin wax and water, while the two other levels show only paraffin wax temperature. At the upper level, the temperature of paraffin wax is higher than the water temperature because of the solar radiation intensity exposed directly to the surface of the copper plate between the pipes and passes through it in the form of heat to paraffin wax. While the water at this level is in the center of the pipes at a distance equal to the pipe's radius from the surface of the pipes that are exposed to solar radiation. In addition, it is clear can see the temperature for both water and paraffin wax are at the collector exit is higher than the entrance. Similar behavior for second level. The lowest level, the temperature of paraffin wax and water are equals through the whole domain. At 4:00 PM (in Figure 7(b)), the temperature of water seems higher than the paraffin wax temperature. At 9:00 PM (in Figure 7(c)), the temperature of paraffin wax is higher than the water because of discharge.

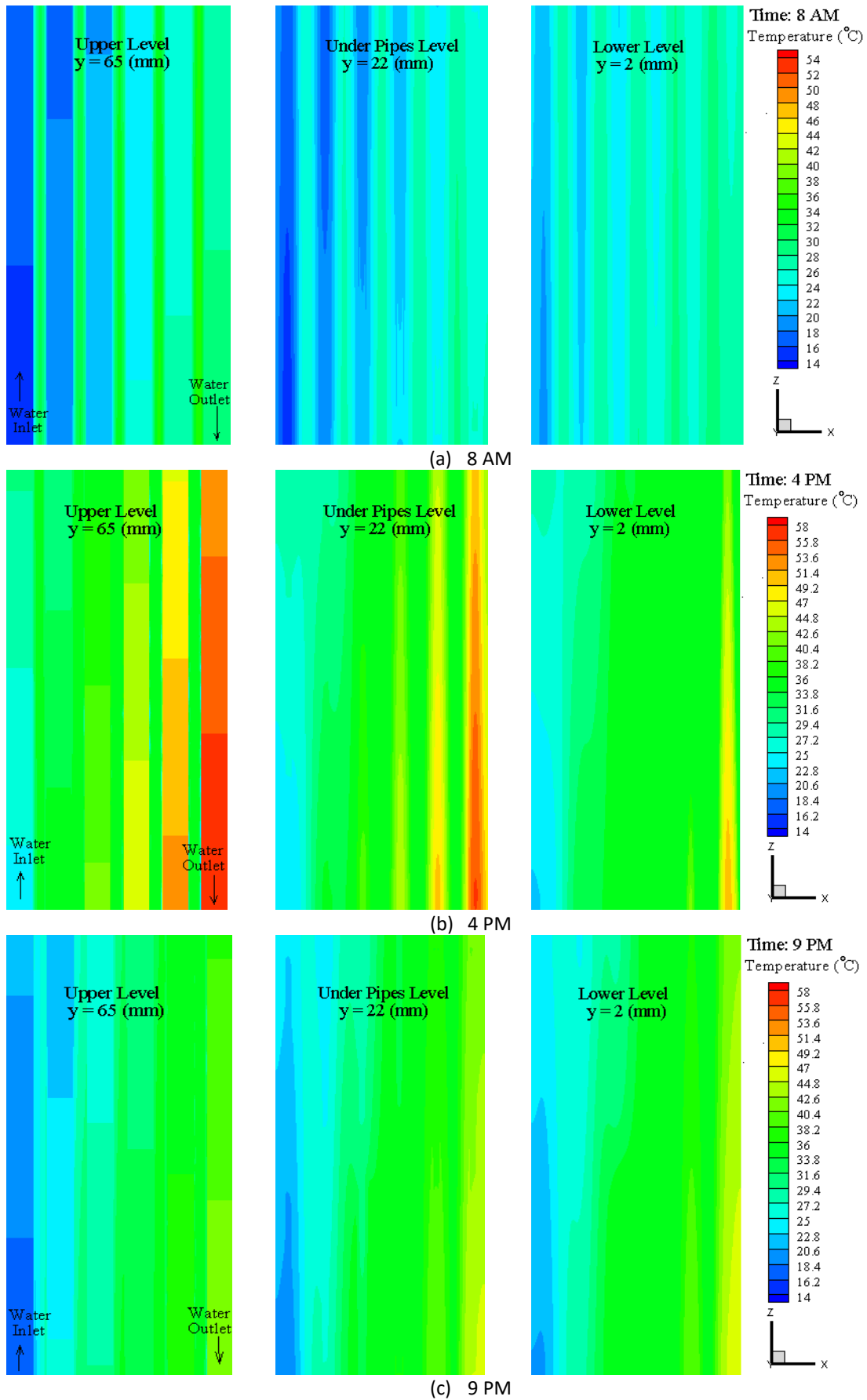


Fig. 7. Contours of the temperature distribution at different time, (a) 8 AM, (b) 4 PM, and (c) 9 PM in (x, z) plane with different levels in y -direction

Figure 8 shows the variation of the average temperature for paraffin wax at a selected point located under the pipes in the direction of water flow from the entrance to the exit. The purpose of this plotting is to represent the behavior change for both water and paraffin wax with the daily hours. It is worth mentioning that the paraffin wax temperature increases with increases of solar intensity at day hours (charging), then as the night hours the paraffin wax temperature decreases under the lower pipes and increases under the upper pipes, after this slowly decreased with increasing of the time, that is because of the heat energy stored in the paraffin wax is moved to the up according to the effect of convection inside the paraffin wax. It is concluded from the graph of Figure 8, that the average temperature of paraffin wax has reached the required temperature (34 °C) at all times except time (8:00 AM), this means that the paraffin wax is capable to charge the water with the required energy during the night.

Figure 9 represents the comparison between the experimental results from the previous work and the predicted CFD results of the present work for the temperature variation in the time to the paraffin wax at a selected point under the pipe exit. It can be concluded that the predicted results from CFD and experimental work are practically identical to each other in the period from sunrise to noon. It is a notice that in the afternoon time, the experimental results are somewhat higher than the CFD results because of heat is added to the solar collector system from many sources surrounding the experiment such as the floor, walls and the metal structure of the solar collector reflects heat towards the water and wax inside the solar collector. From these results, it is concluded that the CFD results give a good agreement with the experimental results.

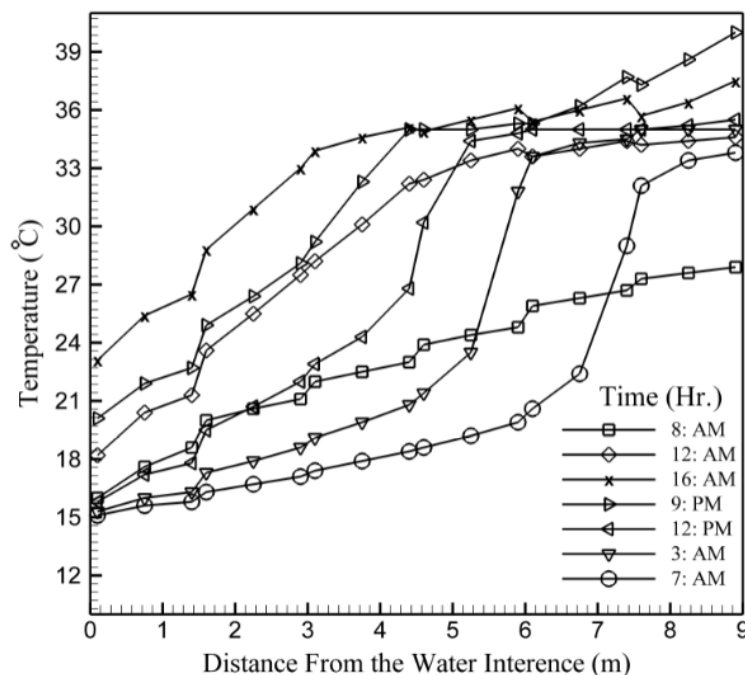


Fig. 8. Variations of average temperature of paraffin wax under the pipes in the direction of water flow from the entrance

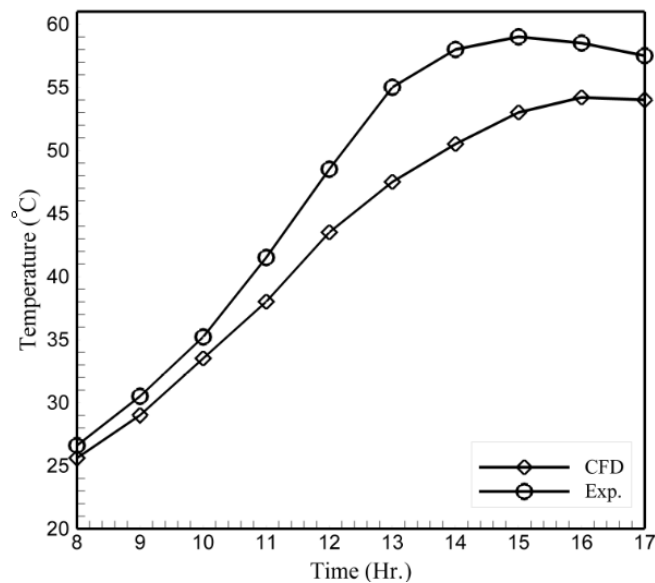


Fig. 9. Comparison between Experimental and CFD results of the temperature with time for the paraffin wax at point under the pipe exit

4. Conclusions

Referring to the previous experimental completed work by the authors for using PCM to improve the heat transfer performance of the solar water collector. In this work, the authors use the CFD tool to investigate numerically the temperature distribution over time of water flow within the solar collector and PCM that placed in the tank at the back of the collector as storage media. The finite volume method with the enthalpy method is also used in this simulation. CFD was conducted during the simulation and the concluded from the simulation show that the maximum temperature of the water outlet is (58 °C) at (4:00 pm), while the maximum temperature of PCM is (54 °C) at (5:00 pm). Over daylight hours, water temperature is higher than that of PCM (PCM charge). The PCM discharge started at the time (5:30 pm) until late time until the night, and the calculated temperature of the PCM at the exit is capable to charge the water with the required temperature of 34 °C during the night. It is noticed that the predicted results from the CFD give good agreement with the experimental results founded previously, therefore the CFD tool is capable to show the complete temperature distribution in the PCM (paraffin wax) during the day and it is able to solve the problem with different parameters related to PCM (different properties).

5. Recommendations and Future Work

The authors recommended using an extension of the present experimental and numerical research for the future work. The following points are recommended for the additional study in this field.

- i. Studying experimentally and numerically the effect of using different PCM for the same current solar collector system.
- ii. Studying experimentally using the porous media with PCM for the same present solar collector system.
- iii. Studying experimental work for the vertical pipes of the solar collector system rather than the horizontal pipes used in the present work.

References

- [1] Hasan, Hiba A., and Ihsan Y. Hussain. "EXPERIMENTAL INVESTIGATION OF THERMAL PERFORMANCE ENHANCEMENT OF CASCADE THERMAL ENERGY STORAGE SYSTEM BY USING METAL FOAM." *International Journal of Mechanical Engineering and Technology* 9, no. 9 (2018): 1537-1549.
- [2] Chiu J. "Latent heat thermal energy storage for indoor comfort control." Ph.D. Thesis, KTH School of Industrial Engineering and Management, 2013.
- [3] Sharma, S. Dutt, and Kazunobu Sagara. "Latent heat storage materials and systems: a review." *International Journal of Green Energy* 2, no. 1 (2005): 1-56.
- [4] Hasan, Hiba A., and Ihsan Y. Hussain. "Theoretical formulation and numerical simulation of thermal performance enhancements for cascade thermal energy storage systems." In *IOP Conference Series: Materials Science and Engineering*, vol. 433, no. 1, p. 012043. IOP Publishing, 2018.
- [5] Jalil, Jalal M., Hassan K. Abdullah, and Kadhim H. Safar. "A Numerical and Experimental Investigation into the Melting of Ice Around a Horizontal Cylinder." (2007).
- [6] Reddy, K. S. "Thermal modeling of PCM-based solar integrated collector storage water heating system." *Journal of Solar Energy Engineering* 129, no. 4 (2007): 458-464.
- [7] Prakash, J., H. P. Garg, and G. Datta. "A solar water heater with a built-in latent heat storage." *Energy conversion and management* 25, no. 1 (1985): 51-56.
- [8] Raed S. Oda, Saleh E. Najim, and Jalal M. Jalil. "Experimental Study of the Thermal Performance of a Solar Collector combined with Paraffin Wax as a Phase Change Material PCM." *International Journal of Engineering Research & Technology* 6, no. 10 (2017): 108-113.
- [9] Hu, Yue, Per Kvols Heiselberg, Hicham Johra, and Rui Guo. "Experimental and numerical study of a PCM solar air heat exchanger and its ventilation preheating effectiveness." *Renewable Energy* 145 (2020): 106-115.
- [10] Vikram, D., S. Kaushik, V. Prashanth, and N. Nallusamy. "An improvement in the solar water heating systems by thermal storage using phase change materials." In *ASME 2006 International Solar Energy Conference*, pp. 409-416. American Society of Mechanical Engineers Digital Collection, 2006.
- [11] El-Sebaei, A. A., A. A. Al-Ghamdi, F. S. Al-Hazmi, and Adel S. Faidah. "Thermal performance of a single basin solar still with PCM as a storage medium." *Applied Energy* 86, no. 7-8 (2009): 1187-1195.
- [12] Koca, Ahmet, Hakan F. Oztop, Tansel Koyun, and Yasin Varol. "Energy and exergy analysis of a latent heat storage system with phase change material for a solar collector." *Renewable Energy* 33, no. 4 (2008): 567-574.
- [13] Chen, Zhenqian, Mingwei Gu, and Donghua Peng. "Heat transfer performance analysis of a solar flat-plate collector with an integrated metal foam porous structure filled with paraffin." *Applied Thermal Engineering* 30, no. 14-15 (2010): 1967-1973.
- [14] Wu, Wei, Suzhou Dai, Zundi Liu, Yiping Dou, Junye Hua, Mengyang Li, Xinyu Wang, and Xiaoyu Wang. "Experimental study on the performance of a novel solar water heating system with and without PCM." *Solar Energy* 171 (2018): 604-612.
- [15] De Gracia, A., E. Oró, M. M. Farid, and L. F. Cabeza. "Thermal analysis of including phase change material in a domestic hot water cylinder." *Applied Thermal Engineering* 31, no. 17-18 (2011): 3938-3945.
- [16] Khot, S. A. "Enhancement of thermal storage system using phase change material." *Energy Procedia* 54, no. 1 (2014): 142-151.
- [17] Redzuan, M., C. L. Saw, W. C. Lew, C. G. Choong, S. Salvinder, H. H. Al-Kayiem, and A. Lukmon. "Numerical simulation of pcm intergrated solar collector storage water heater." *ARPN Journal of Engineering and Applied Sciences* 12, no. 10 (2017): 3363-3367.
- [18] Prakash, Jyoti, Daryn Roan, Wajeha Tauqir, Hassan Nazir, Majid Ali, and Arunachala Kannan. "Off-grid solar thermal water heating system using phase-change materials: design, integration and real environment investigation." *Applied energy* 240 (2019): 73-83.
- [19] Bazri, Shahab, Irfan Anjum Badruddin, Mohammad Sajad Naghavi, Ong Kok Seng, and Somchai Wongwises. "An analytical and comparative study of the charging and discharging processes in a latent heat thermal storage tank for solar water heater system." *Solar Energy* 185 (2019): 424-438.
- [20] Sidik, Nor Azwadi Che, Tung Hao Kean, Hoong Kee Chow, Aravinthan Rajaandra, Saidur Rahman, and Jesbains Kaur. "Performance enhancement of cold thermal energy storage system using nanofluid phase change materials: a review." *International Communications in Heat and Mass Transfer* 94 (2018): 85-95.
- [21] Kean, Tung Hao, and Nor Azwadi Che Sidik. "Thermal performance analysis of nanoparticles enhanced phase change material (NEPCM) in cold thermal energy storage (CTES)." *CFD Letters* 11, no. 4 (2019): 79-91.
- [22] Ahmad Tajuddin Mohamad, Nor Azwadi Che Sidik, M'hamed Beriache. "Thermo Physical Enhancement of Advanced Nano-Composite Phase Change Material." *Journal of Advanced Research in Applied Mechanics* 54, no. 1 (2019): 1-8.

-
- [23] Rathore, Pushpendra Kumar Singh. "An experimental study on solar water heater integrated with phase change material." In *Advances in Fluid and Thermal Engineering*, pp. 347-356. Springer, Singapore, 2019.
- [24] Bouhal, T., T. El Rhafiki, Tarik Kousksou, A. Jamil, and Youssef Zeraouli. "PCM addition inside solar water heaters: Numerical comparative approach." *Journal of Energy Storage* 19 (2018): 232-246.
- [25] Khalifa, Abdul Jabbar N., Kadhim H. Suffer, and Mahmoud Sh Mahmoud. "A storage domestic solar hot water system with a back layer of phase change material." *Experimental Thermal and Fluid Science* 44 (2013): 174-181.
- [26] Cao, Yiding, Amir Faghri, and Won Soon Chang. "A numerical analysis of Stefan problems for generalized multi-dimensional phase-change structures using the enthalpy transforming model." *International journal of heat and mass transfer* 32, no. 7 (1989): 1289-1298.